Carbon 118 (2017) 268–277

Contents lists available at ScienceDirect

Carbon

journal homepage: www.elsevier.com/locate/carbon

# Laser ignition and controlled explosion of nanoenergetic materials: The role of multi-walled carbon nanotubes

Ji Hoon Kim [a, 1], Myung Hoon Cho [a, 1], Kyung Ju Kim [a], Soo Hyung Kim [a, b, *]

[a] Department of Nano Fusion Technology, College of Nanoscience and Nanotechnology, Pusan National University, 30 Jangjeon-dong, Geumjung-gu, Busan 609-735, Republic of Korea

[b] Department of Nano Energy Engineering, College of Nanoscience and Nanotechnology, Pusan National University, 30 Jangjeon-dong, Geumjung-gu, Busan 609-735, Republic of Korea

ARTICLE INFO

*Article history:*
Received 4 November 2016
Received in revised form
22 February 2017
Accepted 15 March 2017

ABSTRACT

Laser irradiation permits the remote ignition of nanoenergetic materials (nEMs). To reliably ignite nEMs with lower-power laser irradiation, light-sensitive materials could be added to the nEMs matrix. In this study, we investigated the effects of multi-walled carbon nanotubes (MWCNTs) on the combustion and explosion characteristics of laser irradiation-ignited nEMs. The threshold power and delay time of ignition gradually decreased with increases in the MWCNT contents of Al nanoparticle (NP)/CuO NP-based nEMs. The threshold power and delay time of MWCNT (10 wt%)/Al NP/CuO NP ignition were reduced to ~40% and ~50%, respectively, of those of MWCNT (0 wt%)/Al NP/CuO NP. This suggests that the MWCNTs act as effective optical igniters by absorbing irradiated laser beams and subsequently generating heat by the photo-thermal effect, promoting nEMs ignition. The optimal addition of $\leq$2 wt% MWCNTs in the nEMs matrix enhanced the pressurization rate, flame propagation speed, and pressure wave speed of nEMs because the MWCNTs rapidly transferred heat energy from nEMs combustion. However, adding excess MWCNTs suppressed the combustion and explosion characteristics of the Al NP/CuO NP-based nEMs matrix by heat dissipation and thermochemical interventions. This suggests that MWCNTs can potentially control the combustion and explosion characteristics of Al NP/CuO NP-based nEMs.



## 1. Introduction

Nanoenergetic materials (nEMs) have internal chemical energy that can be rapidly turned into heat energy upon ignition by an external threshold energy input [1–3]. Various traditional means have been used to ignite nEMs, such as mechanical impaction, friction, electrical sparking, resistive hot wires, and flame [4–8], but these methods require direct contact between the igniter and nEMs. This can impede potential applications of nEMs in various thermal engineering systems.

With the advantages of remote ignition and decreased sensitivity to environmental factors (e.g., temperature, pressure, and humidity), optical means are often employed for the ignition and combustion of nEMs. Many research groups have demonstrated that nEMs can be ignited by optical means, including flash and laser beam irradiation [9–20]. Since the light energy of a flash is not easily focused on a targeted area, the flash has limited use for igniting nEMs under close contact. Unlike the flash, a laser beam focuses light energy such that it can be used to remotely ignite nEMs at a distance, as long as the energy intensity meets the ignition threshold. However, the laser beam intensity is increasingly attenuated with increasing distance between the laser source and nEMs. The laser power must be increased to reliably ignite nEMs from a distance.

An alternative approach for effectively igniting nEMs at lower laser beam intensities is the addition of light-sensitive materials to a nEM matrix. Even with a relatively low-intensity laser beam, suitable optical igniters in the nEM matrix can be easily initiated by absorbing the irradiated laser beam to propagate local ignition heat instantaneously to the neighboring nEMs and thereby trigger

* Corresponding author. Department of Nano Fusion Technology, College of Nanoscience and Nanotechnology, Pusan National University, 30 Jangjeon-dong, Geumjung-gu, Busan 609-735, Republic of Korea.
*E-mail address:* sookim@pusan.ac.kr (S.H. Kim).

[1] Both J. H. Kim and M. H. Cho equally contributed to this work as the first authors.

http://dx.doi.org/10.1016/j.carbon.2017.03.050
0008-6223/

subsequent macroscale combustion. Many research groups have studied carbon nanotubes (CNTs) as potential optical igniters. They observed that CNTs could absorb light energy, vibrate surrounding air molecules, and subsequently generate and rapidly transfer heat through the CNT medium, by the so-called photothermal effect [21–24]. Several groups have employed CNTs for feasibility tests as optical igniters for nEMs under flash irradiation [9–14]. However, the role of CNTs embedded in the nEM matrix ignited by laser beam irradiation has been rarely explored. In this work, we systematically examine the effect of multi-walled carbon nanotubes (MWCNTs) as an optical igniter and heat transfer medium on the laser ignition and explosion characteristics of nEMs. Specifically, we employ an nEM matrix composed of Al nanoparticles (Al NPs) as a fuel and CuO NPs as an oxidizer in this approach.

## 2. Experimental

### 2.1. Materials fabrication

Commercially available Al NPs and Cu NPs were purchased from NT Base Inc., Korea. Al NPs with the average particle size of ~80 nm were used as a fuel without further treatment. CuO NPs as oxidizers with the average particle size of ~152 nm were fabricated by heat-treating Cu NPs at 350 °C for 1 h in air. MWCNTs (CNT Co., Korea) with an average diameter of ~23 nm and a length distribution of 1–25 μm were used as both the optical igniters and explosion control medium. We fabricated MWCNT/Al NP/CuO NP composite powders to examine the characteristics of ignition and explosion by laser beam irradiation, as shown in Fig. 1. Briefly, the Al and CuO NPs were mixed in an ethanol (EtOH) solution at the ratio of Al:CuO = 30:70 wt%, which was previously found to be the optimized mixing condition for occurring the strongest explosive reactivity when they are ignited [8]. The MWCNTs were then added at 1, 2, 5, and 10 wt% to the dispersed Al and CuO NP precursor solution. To homogeneously mix MWCNT/Al NP/CuO NP in the EtOH solution, ultrasonication was performed at 200 W and 40 kHz for approximately 30 min. The EtOH was evaporated in a convection oven at 80 °C for 30 min to obtain the dried MWCNT/Al NP/CuO NP composite powders.

### 2.2. Materials characterization

The physical structures and chemical compositions of the MWCNT/Al NP/CuO NP composites fabricated in this study were characterized by field emission scanning electron microscopy (FESEM; Model S4700, Hitachi) operated at 15 kV, scanning transmission electron microscopy (STEM; Model JEM-2100, JEOL) operated at 200 kV, and X-ray diffractometry (XRD; Model Empyrean series2, PANalytical) using Cu Kα radiation. To examine the thermal properties of the MWCNT/Al NP/CuO NP composites, a series of analyses by thermal gravimetric and differential scanning calorimetry (TG-DSC; Model LABSYS evo, Setaram) were performed at temperatures ranging from 30 °C to 1000 °C at a heating rate of 10 °C·min$^{-1}$ under $N_2$ flow.

### 2.3. Laser ignition and explosion characterization of reacting materials

To investigate the effect of MWCNTs on the laser ignition and explosion characteristics of nEMs, we performed a series of laser ignition tests for various MWCNT/Al NP/CuO NP composites. Briefly, 15 mg of MWCNT/Al NP/CuO NP composite powder was placed on a glass slide and ignited by a continuous-wave green

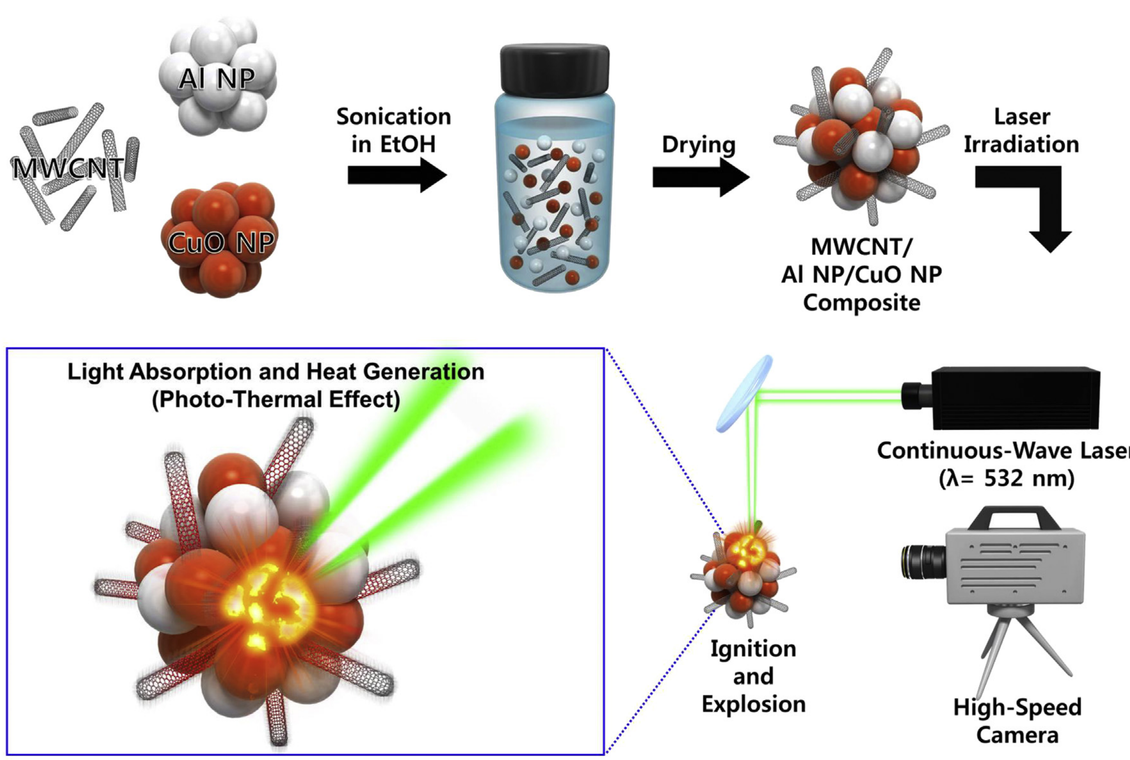


**Fig. 1.** Schematic of laser ignition of MWCNT/Al NP/CuO NP composite powders. (A colour version of this figure can be viewed online.)

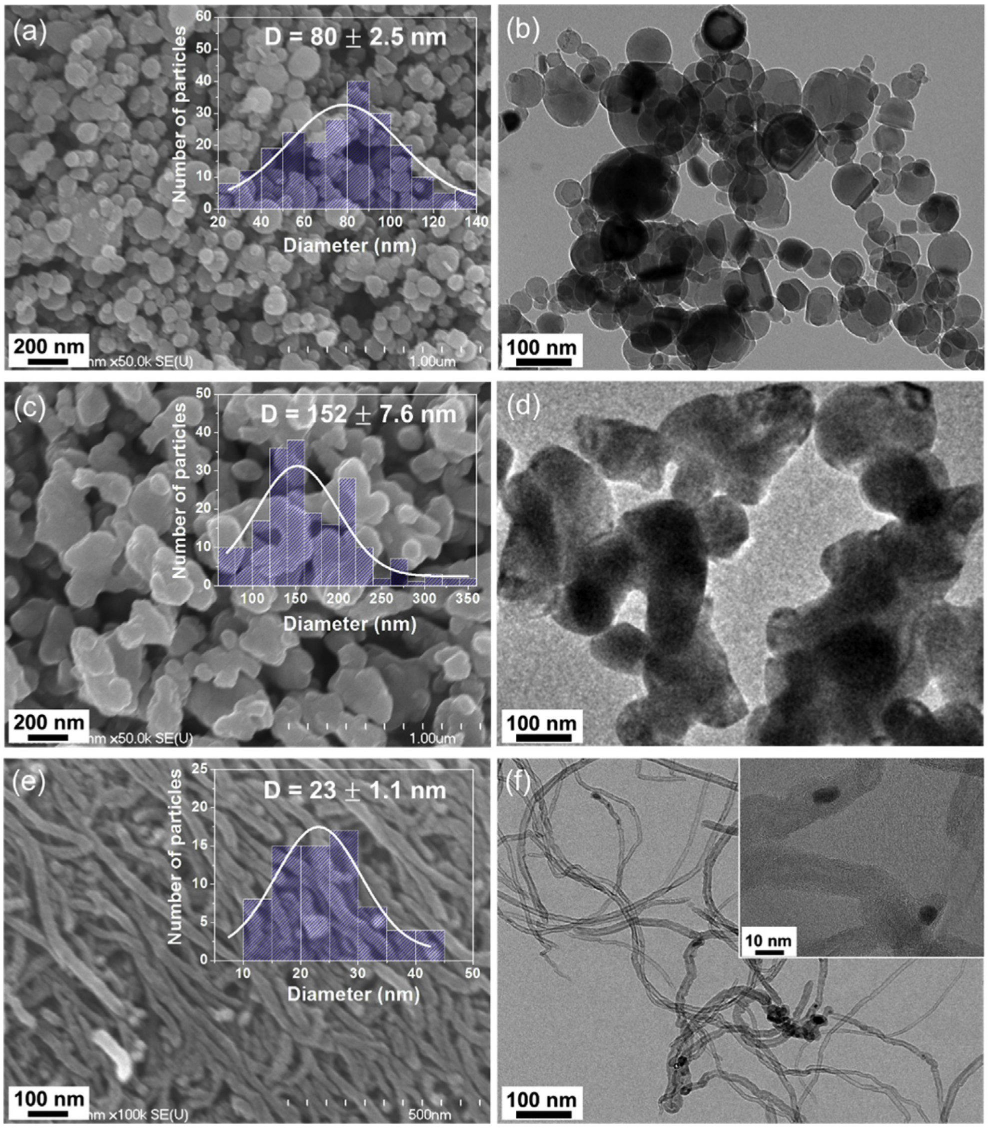


**Fig. 2.** (a) SEM and TEM images of (a, b) Al NPs, (c, d) CuO NPs and (e, f) MWCNTs employed in this study. Insets show the size distribution of particles and MWCNTs. (A colour version of this figure can be viewed online.)

laser beam (wavelength: 532 nm, power range: ~0–1286 mW, beam diameter: 2.5 mm, Model SDL-532-1000T, Shanghai Dream Lasers Technology). The ignition and combustion processes for the various MWCNT (0, 1, 2, 5 and 10 wt%)/Al NP/CuO NP composite powders were recorded using a high-speed camera (Model FASTCAM SA3 120 K, Photron) at a frame rate of 30 kHz. In addition, a pressure cell tester (PCT) was used to measure the pressure trace of the MWCNT/Al NP/CuO NP composites over time [8,25,26]. The MWCNT/Al NP/CuO NP composite powders fabricated were placed in a closed pressure cell with a constant volume of ~13 mL. The powders were then ignited by vertically incident continuous-wave 1 W green laser beam through a glass window. The explosion pressure generated by the laser ignition was measured by a piezoelectric pressure sensor (Model 113A03, PCB Piezotronics) attached to the pressure cell. Simultaneously, the detected pressure signal was amplified and transformed into a voltage signal through a combination of an in-line charge amplifier (Model 422E11, PCB Piezotronics) and signal conditioner (Model 480C02, PCB Piezotronics). Finally, the signal was detected and recorded by a digital oscilloscope (Model TDS 2012B, Tektronix).

To examine the propagation characteristics of the flame and pressure wave generated by the laser ignition of MWCNT/Al NP/CuO NP composites, a series of burn tube tests were conducted [27–30]. Polyethylene terephthalate (PETE) tubes of 3 mm in diameter and 70 mm in length were filled with ~200 mg MWCNT/Al NP/CuO NP composite powder, indicating a packing density of ~0.18 g cm$^{-3}$ and ~30% theoretical density. The cylindrical tubes were inserted into a transparent acrylic block equipped with two piezoelectric pressure sensors (Model 113A03, PCB Piezotronics). Small pressure ports (<1 mm) in the PETE tubes were aligned with the pressure sensors in the acrylic block. Vacuum grease was applied to the joints and connections of the pressure sensors for sealing and thermally insulating them

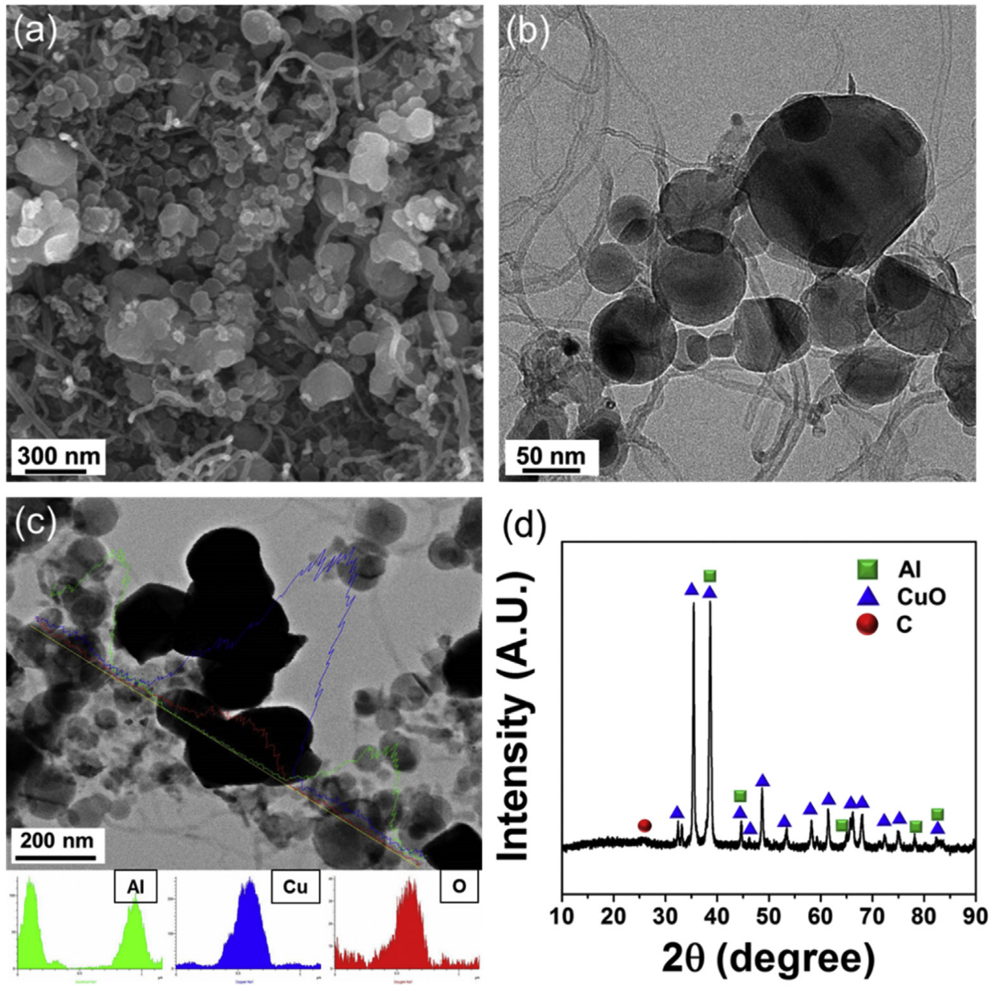


**Fig. 3.** (a) SEM, (b) TEM, (c) STEM, and (d) XRD analyses of MWCNT (5 wt%)/Al NP/CuO NP composite powder. (A colour version of this figure can be viewed online.)

against high reaction temperatures. After igniting the composite powders with laser beam irradiation, the signal detected by the pressure sensors was rapidly processed by the signal conditioner (Model 480C02, PCB Piezotronics) and digital oscilloscope (Model TDS 2012B, Tektronix). The propagation speed of the pressure wave was determined by dividing the distance (~5 cm) between the pressure sensors by the time difference in signal arrival ($\Delta t$). The arrival times were determined as the points of first rise for each pressure sensor (see Fig. 6a). The flame propagation speed was recorded using a high-speed camera at a frame rate of 30 kHz.

## 3. Results and discussion

Fig. 2 presents SEM and TEM images of the Al NPs, CuO NPs, and MWCNTs used in this study. Spherical Al NPs with average diameters of ~80 ± 2.5 nm are observed in Fig. 2a and b. CuO NPs with average diameters of ~152 ± 7.6 nm are highly aggregated and partially coalesced from the heat treatment of Cu NP oxidation, as shown in Fig. 2c and d. The MWCNTs employed in this study contain ~20 walls, a hollow core with an outer diameter of ~23 ± 1.1 nm, and a length distribution of 1–25 μm.

Fig. 3a presents an SEM image of the fabricated MWCNT (5 wt %)/Al NP/CuO NP composite powder. The exposed MWCNTs are homogeneously mixed with Al and CuO NPs. TEM and STEM analyses, as shown in Fig. 3b and c, depict that MWCNTs, Al NPs, and CuO NPs are located in proximity at the nanoscale. This suggests that the simple ultrasonication mixing process for the MWCNT/Al NP/CuO NP colloidal solution is effective to create a homogeneous mixture of the reactants.

In addition, the XRD pattern presents very strong peaks corresponding to Al and CuO, as shown in Fig. 3d. Here, the diffraction peaks for MWCNTs are weak because of the small fraction of MWCNTs. (The XRD patterns of the pure MWCNTs were obtained and are presented in Fig. S1 as a reference.)

To examine the role of MWCNTs in the Al NP/CuO NP matrix, we performed a series of laser irradiation tests for the as-prepared MWCNT/Al NP/CuO NP composites. The laser ignition characteristics of the MWCNT/Al NP/CuO NP composite powders were monitored using a high-speed camera, which provided useful evidence to determine differences in ignition delay time. The threshold power for laser ignition was determined by irradiating the MWCNT/Al NP/CuO NP composite powders with a continuous-wave green laser beam at various power levels. As

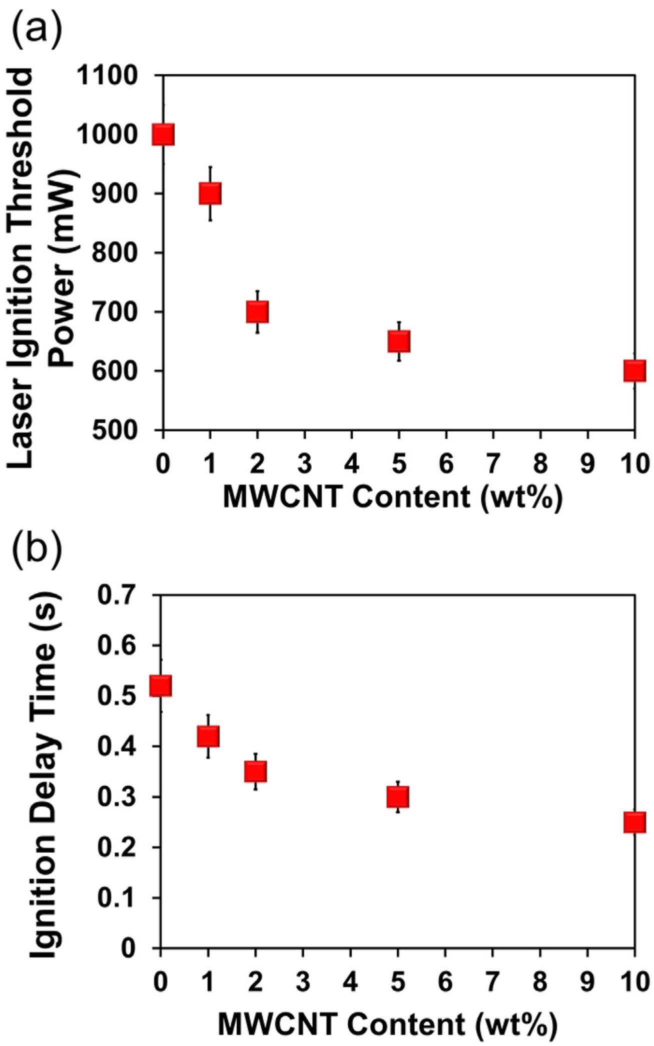


**Fig. 4.** (a) Laser ignition threshold power as a function of MWCNT content, and (b) ignition delay time of MWCNT/Al NP/CuO NP composite powders ignited by the continuous-wave green laser beam irradiation as a function of MWCNT content. (A colour version of this figure can be viewed online.)

the amount of MWCNTs in the Al NP/CuO NP matrix is increased to ~2 wt%, the laser ignition threshold power is decreased, as shown in Fig. 4a. This suggests that a lower-power laser beam is required to reliably ignite composite powders with higher MWCNT contents in the Al NP/CuO NP matrix. The ignition delay time is also decreased with increasing the amount of MWCNT to ~2 wt% in the Al NP/CuO NP matrix, as shown in Fig. 4b. This is because the presence of MWCNTs in the Al NP/CuO NP matrix causes the rapid local ignition of MWCNT/Al NP/CuO NP composites by the photo-thermal effect. However, the addition of more MWCNTs (>2 wt%) has less influence on both the threshold power and delay time of laser ignition. This suggests that excessive amounts of MWCNTs in the Al NP/CuO NP matrix can deteriorate the photo-thermal effect by heat dissipation to the environment by the rapid heat transfer of agglomerated MWCNTs.

To examine the effects of MWCNTs on the explosion pressure of MWCNT/Al NP/CuO NP composites ignited by laser irradiation, the PCT is used as shown in Fig. 5a and b. A fixed mass of ~13 mg of the MWCNT/Al NP/CuO NP composite powder was placed in a confined cell with a constant volume of 13 mL, and then ignited by the vertical irradiation of a continuous-wave 1 W green laser beam through the glass window.

Fig. 5c and d shows the pressure traces and pressurization rates of the MWCNT/Al NP/CuO NP composite powders, respectively. Here, the pressurization rates are calculated as the ratio of the maximum pressure to the rise time. The maximum pressure and pressurization rate both occur in the MWCNT (1 wt%)/Al NP/CuO NP composite. However, when the amount of MWCNTs is increased to >2 wt% in the Al NP/CuO NP matrix, the resulting pressurization rates are significantly decreased. This suggests that the presence of MWNCTs in the Al NP/CuO NP matrix strongly affects the explosion processes of nEMs by interfering with heat transfer and thermochemical properties of the Al NP/CuO NP matrix.

To examine the effect of MWCNTs on the combustion characteristics of MWCNT/Al NP/CuO NP composite powders, a series of burn tube tests were also performed. Fig. 6a and b presents the photograph and schematics of the burn tube test system, respectively. The MWCNT/Al NP/CuO NP composite powders were placed in a thin cylindrical burn tube and then ignited by laser irradiation at one end. The pressure-sensing system comprised two piezoelectric pressure sensors, a signal conditioner, and a digital oscilloscope for analyzing pressure propagation. In addition, a high-speed camera system was installed to record the flame front propagation in the burn tubes. Fig. 6c shows photographs of the flame propagation of the various MWCNT/Al NP/CuO NP composite powders ignited in the burn tube. The Al NP/CuO NP composite powder without MWCNTs (i.e., MWCNT (0 wt%)/Al NP/CuO NP) shows a very large bright flame with a blunt front when ignited. This suggests that exothermic heat accumulates at the reaction zone without rapid propagation to the unreacted zone. However, the MWCNT (1 & 2 wt%)/Al NP/CuO NP composite powder shows a very narrow and sharp flame shape and much faster flame propagation than that seen in the MWCNT (0 wt%)/Al NP/CuO NP composite. This is because the heat transfer rate of the MWCNT (1 & 2 wt%)/Al NP/CuO NP composite is considerably enhanced by the incorporation of highly conductive MWCNTs (thermal conductivity of MWCNT, $K_{MWCNT}$ = ~3000 W $m^{-1}\cdot K^{-1}$) in the Al ($K_{Al}$ = ~250 W $m^{-1}\cdot K^{-1}$)/CuO ($K_{CuO}$ = ~30 W $m^{-1}\cdot K^{-1}$) matrix [31–42]. Thus, the combustion heat generated is rapidly transferred to the unreacted zone through the MWCNT medium, which increases the flame propagation speed. However, the flame propagation speed is significantly decreased for amounts of MWCNTs >2 wt% in the Al NP/CuO NP matrix. This suggests that the presence of excessive MWCNTs deteriorates the combustion reaction of nEMs by heat dissipation and thermochemical interference.

The explosion pressures of the MWCNT/Al NP/CuO NP composite powders ignited in the burn tubes were measured by pressure-sensing systems attached to the burn tubes, as shown in Fig. 7a–d. The two pressure sensors A and B (see Fig. 6 b) are installed along the burn tube ~5 cm apart. The time difference ($\Delta t$) between pressure signal input at pressure sensors A and B is measured. The propagation speed of the pressure wave generated by the combustion of MWCNT/Al NP/CuO NP composite powders is experimentally determined as the ratio of the pressure sensor distance to $\Delta t$. To determine the flame propagation speed, the flame front position and time are measured by high-speed photography, as shown in Fig. 7e. The flame propagation speed of the MWCNT/Al NP/CuO NP composite powders in the early

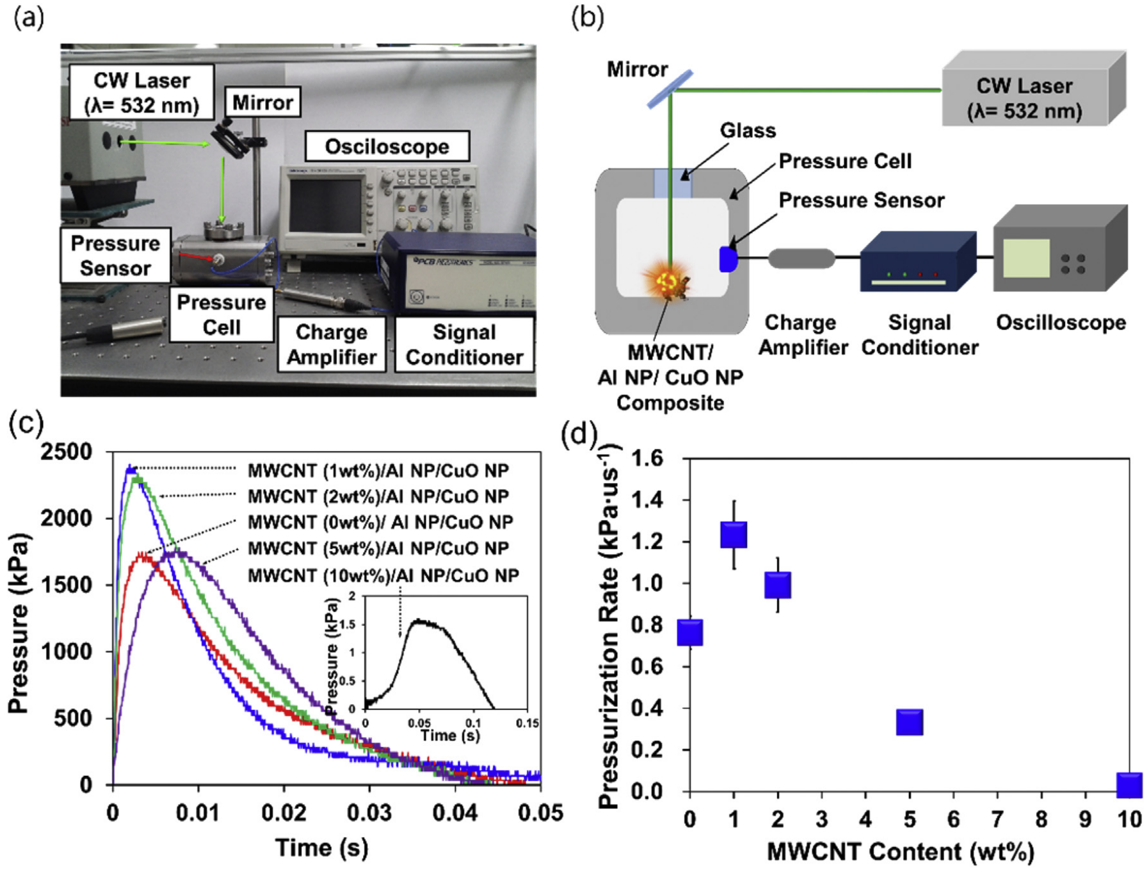


**Fig. 5.** (a) Photograph and (b) schematic of pressure cell tester system, (c) pressure trace, and (d) pressurization rate of MWCNT/Al NP/CuO NP composites ignited by laser irradiation. (A colour version of this figure can be viewed online.)

stage linearly increases before significantly increasing at a point with a steeper increment. This behavior is attributed to the enhancement of convective heat transfer [27–30]. The air within the voids of the loose MWCNT/Al NP/CuO NP composite powders becomes highly heated by the accumulated heat and pressure of the combustion reaction zone. Heat transfer promotes the combustion reaction significantly throughout the MWCNT/Al NP/CuO NP matrix. Based on the high-speed camera snapshots and explosion pressure analyses, the propagation speeds of the flame and pressure waves of various MWCNT/Al NP/CuO NP composites are calculated as shown in Fig. 7f. The highest propagation speeds of the flame and pressure waves are ~236 m $s^{-1}$ and ~446 m $s^{-1}$, respectively, for the MWCNT (1 wt%)/Al NP/CuO NP composite. With an increase in MWCNT contents to exceed 2 wt% in the Al NP/CuO NP matrix, the propagation speeds of both the flame and pressure waves are significantly decreased. This is very similar to the PCT analysis results shown in Fig. 5d, suggesting that the PCT and burn tube tests precisely corroborate the combustion and explosion characteristics of nEMs.

To examine the effect of MWCNTs on the thermal properties of MWCNT/Al NP/CuO NP composite powders, TG-DSC analyses were performed, as shown in Fig. 8. The first exothermic reaction zone commonly occurs in the temperature range of ~400–600 °C and an exothermic peak appears at approximately 540 °C, as shown in Fig. 8a. During the exothermic reaction, the solid Al NPs and CuO NPs thermally react. The total exothermic heat energy is calculated as ~1591 J $g^{-1}$ for the Al NP/CuO NP composite without MWCNTs. With increasing the amount of MWCNTs in the Al NP/CuO NP matrix from 1 wt% to 10 wt%, the total exothermic heat energy is gradually decreased. The second exothermic reaction zone is observed at the temperature range of ~650–800 °C for all samples. This is attributed to the reaction between unreacted melted Al and solid CuO NPs. The endothermic peaks generated by the melted Al NPs are weakly observed at ~660 °C. The clear endothermic reaction of pure Al NPs was confirmed by the TG-DSC analysis for pure Al NPs as shown in Fig. S2a. The pure CuO NPs showed an endothermic peak at ~900 °C, attributed to the reduction of CuO to $Cu_2O$ as shown in Fig. S2b [43,44].

When the MWCNT contents in Al NP/CuO NP composites are increased, the second exothermic peak increases in intensity and simultaneously shifts to lower temperatures. This is because the amount of unreacted Al is increased by the presence of excessive MWCNTs. This suggests that the excessive MWCNTs inhibit the first exothermic reaction between the Al and CuO NPs, with more Al NPs remaining unreacted in the first exothermic reaction. The unreacted Al then participates more actively in the second exothermic reaction between melted Al and solid CuO NPs. This is corroborated by the TG analyses shown in Fig. 8b. The MWCNTs are oxidized by the heat and oxygen generated by the exothermic reaction between Al and CuO NPs in the $N_2$ atmosphere of TG

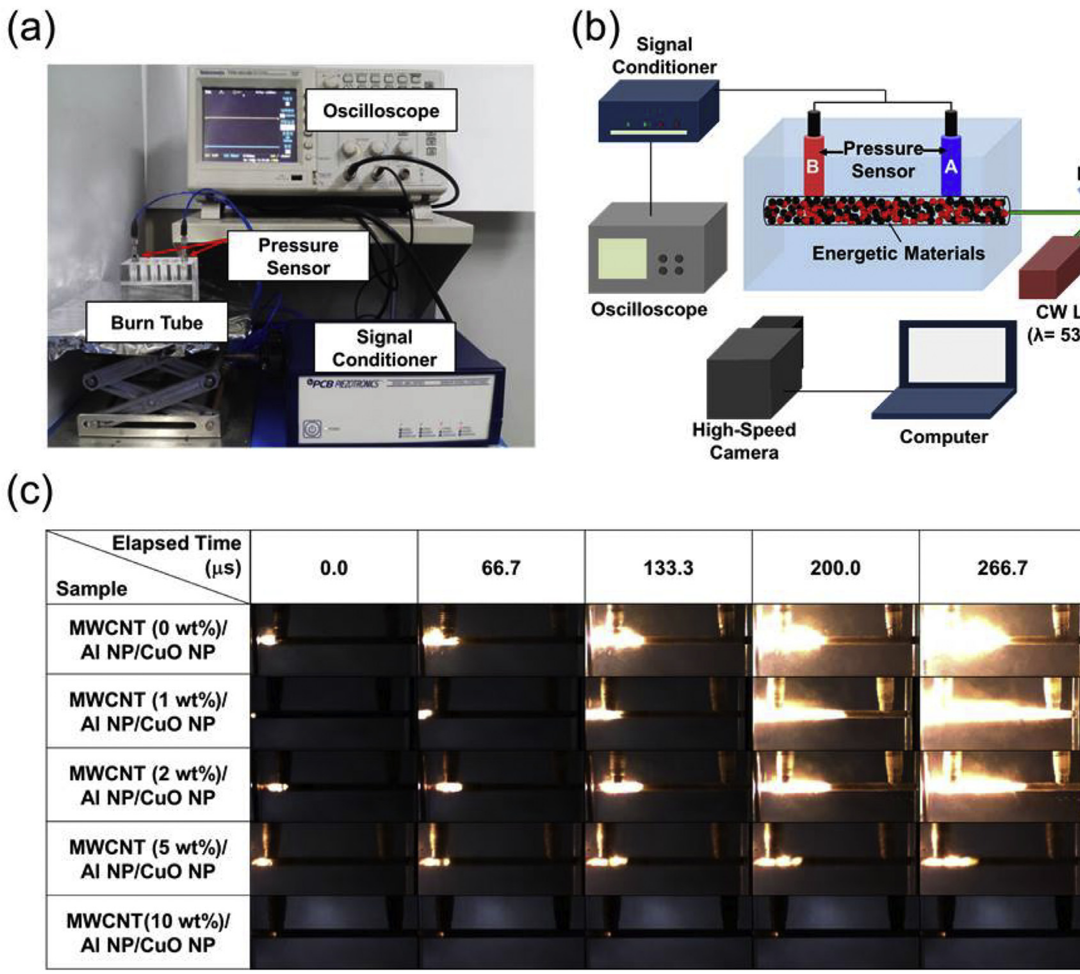


**Fig. 6.** (a) Schematic and (b) photograph of burn tube apparatus, and (c) high-speed camera images of various MWCNT (0, 1, 2, 5 and 10 wt%)/Al NP/CuO NP composites ignited by laser beam irradiation in the burn tubes. (A colour version of this figure can be viewed online.)

analysis. This suggests that the presence of MWCNTs hinders the complete combustion reaction to some extent by intercepting the heat and oxygen from the exothermic reaction of the Al and CuO NP matrix. The appreciable weight losses of MWCNT oxidation occur with the exothermic reaction of the Al NP/CuO NP matrix. In the reaction temperature range of ~400–600 °C, the weight loss of the composites from MWCNT combustion is significantly increased with increases in the MWCNT contents of the composites. This suggests that MWCNTs could act as a controlling medium for combustion and explosion by thermochemical intervention in the exothermic reaction of Al NP/CuO NP composites.

## 4. Conclusions

In this study, we have investigated the effect of the presence of MWCNTs on the laser ignition and explosion characteristics of Al NP/CuO NP-based nEM composites. The MWCNT/Al NP/CuO NP composite powders were fabricated using a simple sonication process in EtOH solution. The thermal energy generated by laser beam irradiation on MWCNTs reliably ignited the Al NP/CuO NP-based nEM composites. Specifically, the threshold power and delay time of laser ignition were significantly reduced by the addition of MWCNTs to the Al NP/CuO NP composites, suggesting that the MWCNTs were effective optical igniters in the Al NP/CuO NP-based nEM matrix. The effect of MWCNTs on the combustion and explosion characteristics of Al NP/CuO NP-based nEM matrix was also examined. The optimal level of $\leq$2 wt% MWCNTs in the nEM matrix enhanced the pressurization rate, flame propagation speed, and pressure wave speed of the nEMs. However, the addition of excessive MWCNTs (>2 wt%) suppressed the combustion and explosion characteristics of the Al NP/CuO NP-based nEM matrix by heat dissipation and thermochemical intervention in the Al/CuO reaction. This suggests that MWCNTs can potentially be used as optical igniters and explosion control media for realizing remote laser ignition and controlled explosions in Al NP/CuO NP-based nEMs.

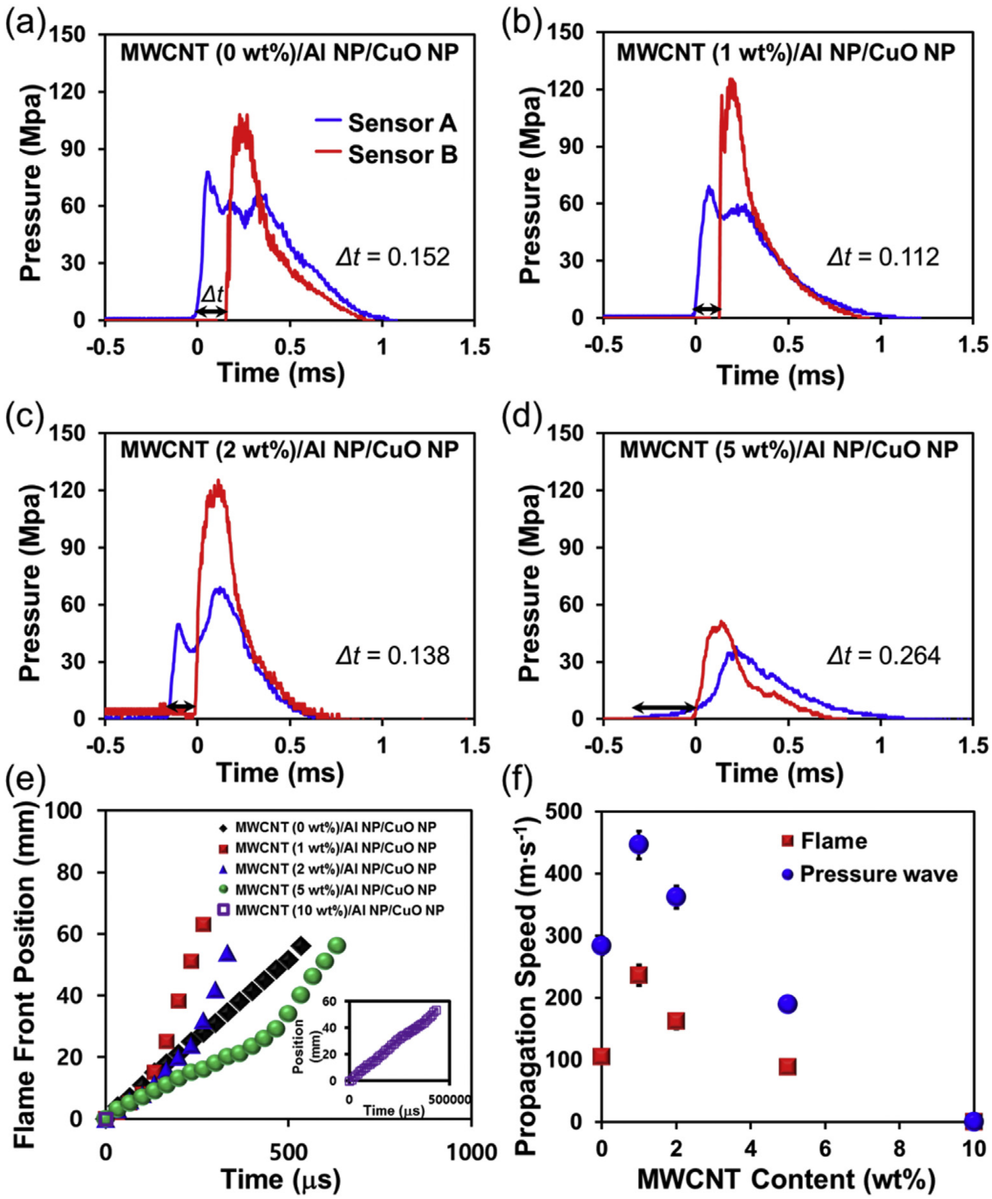


**Fig. 7.** Pressure traces of (a) MWCNT (0 wt%)/Al NP/CuO NP, (b) MWCNT (1 wt%)/Al NP/CuO NP, (c) MWCNT (2 wt%)/Al NP/CuO NP, and (d) MWCNT (5 wt%)/Al NP/CuO NP composites ignited by laser beam irradiation. (e) Flame front positions of various MWCNT (0, 1, 2, 5 and 10 wt%)/Al NP/CuO NP composites as a function of time, and (f) the average flame and pressure wave propagation speeds of various MWCNT (0, 1, 2, 5 and 10 wt%)/Al NP/CuO NP composites ignited in the burn tubes. (A colour version of this figure can be viewed online.)

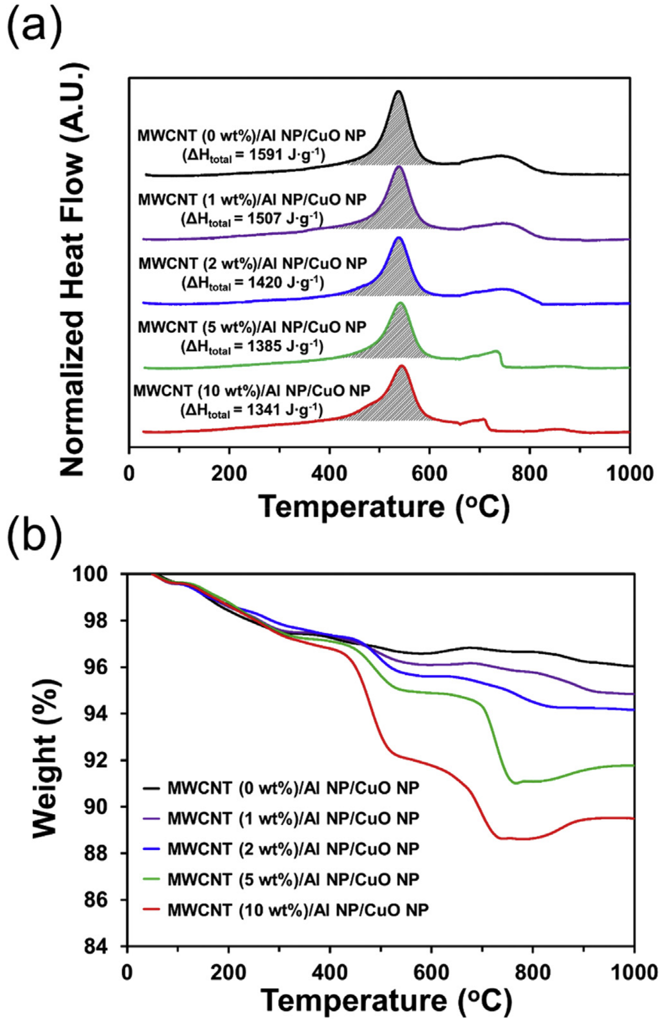


**Fig. 8.** (a) DSC and (b) TG analyses of MWCNT (0, 1, 2, 5 and 10 wt%)/Al NP/CuO NP composite powders. (A colour version of this figure can be viewed online.)

## Acknowledgements

This research was supported by the Civil & Military Technology Cooperation Program through the National Research Foundation of Korea grant funded by the Ministry of Science, ICT and Future Planning (No. 2013M3C1A9055407). This research was also partially supported by the National Research Foundation of Korea grant funded by the Korean government (MSIP) (No. 2015R1A2A1A15054036).

## Appendix A. Supplementary data

Supplementary data related to this article can be found at http://dx.doi.org/10.1016/j.carbon.2017.03.050.

## References

[1] S.H. Kim, M.R. Zachariah, Enhancing the rate of energy release from nanoenergetic materials by electrostatically enhanced assembly, Adv. Mater. 16 (20) (2004) 1821–1825.
[2] J.Y. Ahn, W.D. Kim, J.H. Kim, J.H. Kim, J.K. Lee, J.M. Kim, et al., Gas-phase synthesis of bimetallic oxide nanoparticles with designed elemental compositions for controlling the explosive reactivity of nanoenergetic materials, J. Nanomater. 2011 (2011) 42.
[3] C. Wu, K. Sullivan, S. Chowdhury, G. Jian, L. Zhou, M.R. Zachariah, Encapsulation of perchlorate salts within metal oxides for application as nanoenergetic oxidizers, Adv. Funct. Mater. 22 (1) (2012) 78–85.
[4] D. Skinner, D. Olson, A. Block-Bolten, Electrostatic discharge ignition of energetic materials, Prop. Explos. Pyrotech. 23 (1997) 34–42.
[5] E.M. Hunt, S. Malcolm, M.L. Pantoya, F. Davis, Impact ignition of nano and micron composite energetic materials, Int. J. Impact Eng. 36 (6) (2009) 842–846.
[6] A.N. Ali, S.F. Son, B.W. Asay, R.K. Sander, Importance of the gas phase role to the prediction of energetic material behavior: an experimental study, J. Appl. Phys. 97 (6) (2005) 063505.
[7] M.H. Wu, M.P. Burke, S.F. Son, R.A. Yetter, Flame acceleration and the transition to detonation of stoichiometric ethylene/oxygen in microscale tubes, Proc. Combust. Inst. 31 (2) (2007) 2429–2436.
[8] J.Y. Ahn, W.D. Kim, K. Cho, D. Lee, S.H. Kim, Effect of metal oxide nanostructures on the explosive property of metastable intermolecular composite particles, Powder Technol. 211 (1) (2011) 65–71.
[9] J.H. Kim, J.Y. Ahn, H.S. Park, S.H. Kim, Optical ignition of nanoenergetic materials: the role of single-walled carbon nanotubes as potential optical igniters, Combust. Flam. 160 (4) (2013) 830–834.
[10] J.H. Kim, S.B. Kim, M.G. Choi, D.H. Kim, K.T. Kim, H.M. Lee, et al., Flash-ignitable nanoenergetic materials with tunable underwater explosion reactivity: the role of sea urchin-like carbon nanotubes, Combust. Flam. 162 (4) (2015) 1448–1454.
[11] X. Xiang, S.B. Xiang, Z. Wang, X. Wang, G. Hua, Photo-responsive behaviors and structural evolution of carbon-nanotube-supported energetic materials under a photoflash, Mater. Lett. 88 (2012) 27–29.
[12] M.R. Manaa, A.R. Mitchell, R.G. Garza, P.F. Pagoria, B.E. Watkins, Flash ignition and initiation of explosives-nanotubes mixture, J. Am. Chem. Soc. 127 (40) (2005) 13786–13787.
[13] C.D. Malec, N.H. Voelcker, J.G. Shapter, A.V. Ellis, Carbon nanotubes initiate the explosion of porous silicon, Mater. Lett. 64 (22) (2010) 2517–2519.
[14] Y. Ohkura, P.M. Rao, X. Zheng, Flash ignition of Al nanoparticles: mechanism and applications, Combust. Flam. 158 (12) (2011) 2544–2548.
[15] J.J. Granier, M.L. Pantoya, Laser ignition of nanocomposite thermites, Combust. Flam. 138 (4) (2004) 373–383.
[16] S.C. Stacy, M.L. Pantoya, Laser ignition of nano-composite energetic loose powder, Propel. Explos. Pyrot. 38 (2013) 441–447.
[17] B.W. Asay, G.W. Laabs, B.F. Henson, D.J. Funk, Speckle photography during dynamic impact of an energetic material using laser-induced fluorescence, J. Appl. Phys. 82 (3) (1997) 1093–1099.
[18] K.C. Lee, K.H. Kim, J.J. Yoh, Modeling of high energy laser ignition of energetic materials, J. Appl. Phys. 103 (2008) 08353608.
[19] Y. Yang, S. Wang, Z. Sun, D.D. Dlott, Near-Infrared and visible absorption spectroscopy of nano-energetic materials containing aluminum and boron, Propel. Explos. Pyrot. 30 (3) (2005) 171–177.
[20] H. Oestmark, N. Roman, Laser ignition of pyrotechnic mixtures: ignition mechanisms, J. Appl. Phys. 73 (4) (1993) 1993–2003.
[21] P.M. Ajayan, M. Terrones, A. De la Guardia, V. Huc, N. Grobert, B.Q. Wei, H. Lezec, et al., Nanotubes in a flash–ignition and reconstruction, Science 296 (5568) (2002), 705–705.
[22] B. Bockrath, J.K. Johnson, D.S. Sholl, B. Howard, C. Matranga, W. Shi, et al., Igniting nanotubes with a flash, Science 297 (5579) (2002) 192–193.
[23] S.H. Tseng, N.H. Tai, W.K. Hsu, L.J. Chen, J.H. Wang, C.C. Chiu, et al., Ignition of carbon nanotubes using a photoflash, Carbon 45 (5) (2007) 958–964.
[24] J. Smits, B. Wincheski, M. Namkung, R. Crooks, R. Louie, Response of Fe powder, purified and as-produced HiPco single-walled carbon nanotubes to flash exposure, Mater. Sci. Eng. A 358 (1) (2003) 384–389.
[25] K. Sullivan, M. Zachariah, Simultaneous pressure and optical measurements of nanoaluminum thermites: investigating the reaction mechanism, J. Propul. Power 26 (3) (2010) 467–472.
[26] A. Prakash, A.V. McCormick, M.R. Zachariah, Synthesis and reactivity of a super-reactive metastable intermolecular composite formulation of Al/$KMnO_4$, Adv. Mater. 17 (7) (2005) 900–903.
[27] B.S. Bockmon, M.L. Pantoya, S.F. Son, B.W. Asay, J.T. Mang, Combustion velocities and propagation mechanisms of metastable interstitial composites, J. Appl. Phys. 98 (6) (2005), 64903–64903.
[28] G.M. Dutro, R.A. Yetter, G.A. Risha, S.F. Son, The effect of stoichiometry on the combustion behavior of a nanoscale Al/$MoO_3$ thermite, Proc. Combust. Inst. 32 (2) (2009) 1921–1928.
[29] J. Shen, Z. Qiao, K. Zhang, J. Wang, R. Li, H. Xu, et al., Effects of nano-Ag on the combustion process of Al–CuO metastable intermolecular composite, Appl. Therm. Eng. 62 (2) (2014) 732–737.
[30] K.W. Watson, M.L. Pantoya, V.I. Levitas, Fast reactions with nano-and micrometer aluminum: a study on oxidation versus fluorination, Combust. Flam. 155 (4) (2008) 619–634.
[31] W. Choi, S. Hong, J.T. Abrahamson, J.H. Han, C. Song, N. Nair, et al., Chemically driven carbon-nanotube-guided thermopower waves, Nat. Mater. 9 (5) (2010) 423–429.
[32] J.T. Abrahamson, N. Nair, M.S. Strano, Modelling the increase in anisotropic reaction rates in metal nanoparticle oxidation using carbon nanotubes as thermal conduits, Nanotechnology 19 (19) (2008) 195701.
[33] M.B. Jakubinek, M.A. White, G. Li, C. Jayasinghe, W. Cho, M.J. Schulz, et al., Thermal and electrical conductivity of tall, vertically aligned carbon nanotube arrays, Carbon 48 (13) (2010) 3947–3952.
[34] W. Lin, J. Shang, W. Gu, C.P. Wong, Parametric study of intrinsic thermal transport in vertically aligned multi-walled carbon nanotubes using a laser

flash technique, Carbon 50 (4) (2012) 1591–1603.
[35] M. Qin, Y. Feng, T. Ji, W. Feng, Enhancement of cross-plane thermal conductivity and mechanical strength via vertical aligned carbon nanotube@graphite architecture, Carbon 104 (2016) 157–168.
[36] L. Qiu, X. Wang, D. Tang, X. Zheng, P.M. Norris, D. Wen, et al., Functionalization and densification of inter-bundle interfaces for improvement in electrical and thermal transport of carbon nanotube fibers, Carbon 105 (2016) 248–259.
[37] Z. Han, A. Fina, Thermal conductivity of carbon nanotubes and their polymer nanocomposites: a review, Prog. Polym. Sci. 36 (7) (2011) 914–944.
[38] A.E. Aliev, M.H. Lima, E.M. Silverman, R.H. Baughman, Thermal conductivity of multi-walled carbon nanotube sheets: radiation losses and quenching of phonon modes, Nanotechnology 21 (3) (2009) 035709.
[39] Q. Zhang, G. Chen, S.F. Yoon, J. Ahn, S.G. Wang, Q. Zhou, et al., Thermal conductivity of multiwalled carbon nanotubes, Phys. Rev. B 66 (16) (2002) 165440.
[40] P. Kim, L. Shi, A. Majumdar, P.L. McEuen, Thermal transport measurements of individual multiwalled nanotubes, Phys. Rev. Lett. 87 (21) (2001) 215502.
[41] D.D.L. Chung, Materials for thermal conduction, Appl. Therm. Eng. 21 (16) (2001) 1593–1605.
[42] M.S. Liu, M.C. Lin, I.T. Huang, C.C. Wang, Enhancement of thermal conductivity with CuO for nanofluids, Chem. Eng. Tech. 29 (1) (2006) 72–77.
[43] P.D. Kirsch, J.G. Ekerdt, Chemical and thermal reduction of thin films of copper (II) oxide and copper (I) oxide, J. Appl. Phys. 90 (8) (2001) 4256–4264.
[44] J. Li, G. Vizkelethy, P. Revesz, J.W. Mayer, K.N. Tu, Oxidation and reduction of copper oxide thin films, J. Appl. Phys. 69 (2) (1991) 1020–1029.